Structure and Dynamics of a Thermoresponsive Microgel around Its Volume Phase Transition Temperature

ARTICLE *in* THE JOURNAL OF PHYSICAL CHEMISTRY B · AUGUST 2010

Impact Factor: 3.3 · DOI: 10.1021/jp100962p · Source: PubMed

Structure and Dynamics of a Thermoresponsive Microgel around Its Volume Phase Transition Temperature

Shivkumar V. Ghugare,[†] Ester Chiessi,[†] Mark T. F. Telling,[‡] Antonio Deriu,[§] Yuri Gerelli,[§] Joachim Wuttke,[||] and Gaio Paradossi*[,†]

Dipartimento di Scienze e Tecnologie Chimiche, Università di Roma Tor Vergata and SOFT, CNR-INFM, Rome, Italy; ISIS Facility, Rutherford Appleton Laboratory, Chilton Didcot, Oxfordshire OX11 0QX, U.K.; Dipartimento di Fisica, Università di Parma, Parma, Italy; and JCNS at FRM II, Forschungszentrum Jülich, 85747 Garching, Germany

Received: February 1, 2010; Revised Manuscript Received: June 18, 2010

Sustained drug delivery requires the use of multifunctional devices with enhanced properties. These properties include responsiveness to external stimuli (such as temperature, pH, ionic strength), ability to deliver suitably designed ligands to specific receptors, enhanced bioadhesion to cells, and cytocompatibility. Microgels represent one of such multifunctional drug delivery devices. Recently, we described the fabrication of a stable colloidal aqueous suspension of cytocompatible microgel spheres based on a poly(vinyl alcohol)/poly(methacrylate-*co*-*N*-isopropylacrylamide) network (Ghugare, S.; Mozetic, P.; Paradossi, G. *Biomacromolecules* **2009**, *10*, 1589). These microgel spheres undergo an entropy-driven volume phase transition around the physiological temperature, this phase transition being driven by the incorporation of NiPAAm residues in the network. In that study, the microgel was loaded with the anticancer drug doxorubicin. As the microgel shrank, a marked increase in the amount of doxorubicin released was noted. Indeed, dynamic light scattering measurements showed the diameter reduction to be about 50%. In the present paper, we focus on some fundamental issues regarding modifications of the hydrogel architecture at a nanoscopic level as well as of the diffusive behavior of water associated with the polymer network around the volume phase transition temperature (VPTT). Sieving and size exclusion effects were studied by laser scanning confocal microscopy with the microgel exposed to fluorescent probes with different molecular weights. Confocal microscopy observations at room temperature and at 40 °C (i.e., below and above the VPTT) provided an evaluation of the variation of the average pore size (from 5 nm to less than 3 nm). Using quasielastic neutron scattering (QENS) with the IRIS spectrometer at ISIS, UK, the diffusive behavior of water molecules closely associated to the polymer network around the VPTT was investigated. A clear change in the values of diffusion coefficient of bound water was observed at the transition temperature. In addition, the local dynamics of the polymer itself was probed using the QENS spectrometer SPHERES at FRM II, Germany. For this study, the microgel was swollen in D_2O. An average characteristic distance of about 5 Å for the localized chain motions was evaluated from the elastic incoherent structure factor (EISF) and from the *Q*-dependence of the Lorentzian width.

Introduction

The role of smart devices for controlling the delivery of drugs is gaining importance in the diagnostic and therapeutic fields because of the remarkable achievements being made in the micro-/nanofabrication of soft matter materials. Such advances not only allow for a more efficient drug administration and delivery but also provide targeted drug delivery via conjugation of the surface of the smart device with suitable ligands. The latter increases the bioavailability of the drug and reduces undesired side effects, so often encountered in cancer chemical therapy.[1,2] Moreover, such colloidal devices exhibit inherent features which are necessary if this therapeutic approach has to be exploited in the field of gene therapy. Such features include hydration to preserve the active conformational state of the macromolecular cargo, as well as cytocompatibility and stealth properties to support transfection.[3] A smart device for drug delivery is able to trigger the release of its payload, in response to external stimuli such as temperature, pH, ionic strength, or a combination of these parameters.[4−7]

The motivation for this work is the design of novel multifunctional polymer-based drug delivery systems and stems from the potential offered by a highly interdisciplinary approach to the development of new materials or tools for therapeutic treatments.[8] Our aim is to fabricate devices with enhanced responsiveness and with suitable surface modifications such that the smart device delivers its pharmacological payload at a specific receptor with greater precision. The efficacy of such devices, which are based on synthetic and natural polymeric materials, is characterized in terms of diffusive processes with time scales covering several decades. As a result, the study of a polymer-based smart device requires a set of experimental methods that enable probing times in the range of nanoseconds to hundreds of seconds. With the availability of high-flux neutron sources, the technique of incoherent quasielastic neutron scattering (QENS) provides a useful method to investigate, and separate, the diffusion of water in the gel matrix and the segmental dynamics of the polymer networks.[9] The space−time

* Corresponding author. E-mail: paradossi@stc.uniroma2.it.
[†] Università di Roma Tor Vergata and SOFT, CNR-INFM.
[‡] Rutherford Appleton Laboratory.
[§] Università di Parma.
[||] Forschungszentrum Jülich.

10.1021/jp100962p
Published on Web 07/26/2010

window accessible to QENS is also easily accessed by molecular dynamics simulations. For example, we recently compared the results of a QENS study on the diffusive behavior of water caged in poly(vinyl alcohol) hydrogels with a detailed analysis of the systems by molecular dynamics simulations.[10−12]

One promising targeted drug delivery device is represented by systems in the form of microgel.[13] This highly hydrated cross-linked polymeric network exhibits features typical of colloidal particles, namely, a high surface/volume ratio, high payload capacity, micrometer-sized dimensions, and enhanced interface exchange. Such characteristics are desirable for sustained drug delivery. Should the microgel also be responsive to external stimuli such as temperature and/or pH changes within physiological ranges, then a volume phase transition can be triggered, enabling the delivery process in a controlled manner.[14−19]

In a previous paper, we obtained a stable, spherically shaped, colloidal microgel with an average diameter of 3 μm based on poly(vinyl alcohol), PVA, using the "water-in-water" microemulsion method.[20] This method avoids the use of organic solvents which very often have a high cytotoxic impact to tissues. Such hydrophilic microgel is supported by a polymer moiety where PVA behaves as bioinert polymer scaffold with suitable water content and poly(methacrylate) chains are the cross-linking elements. The drug loading and release capacities of the microgel were tested by using the anticancer drug doxorubicin.[20] Recently, we incorporated (*N*-isopropylacrylamide) residues into the network while maintaining all the other chemical and structural features.[21] The latter residues promote a volume phase transition[22] at temperatures centered around physiological conditions, thus enabling the possibility of biomedical applications. The cytocompatibility of the system was addressed using a series of tests which evaluated the viability and proliferation of human fibroblasts cells cultured in the presence of the microgel.[21]

In this paper, we address other relevant features of the system, linked to the drug delivery as the microgel internal architecture and the diffusion behavior of water contained in the microgel during the temperature-driven volume phase transition. The structural modifications of the poly(vinyl alcohol)/poly(methacrylate-*co*-*N*-isopropylacrylamide) network affect the pore size and the dynamics of the associated water above and below the volume phase transition temperature, VPTT. These factors are key properties since they act in a concerted manner in drug delivery devices based on stimuli responsiveness.

The structure of poly(*N*-isopropylacrylamide) microgels with an average diameter of 700 nm has been recently characterized.[23,24] In addition, the dynamics of the polymer chains and of water molecules confined in the network around the VPTT has been investigated by QENS and by NMR ^{1}H spin−spin relaxation time experiments, respectively.[25,26] Furthermore, the diffusion processes occurring in monolithic hydrogels (obtained by the cross-linking between telechelic PVA bearing reactive aldehydes as terminal groups) and in microgels based on cross-linked methacryloyl-grafted PVA have been investigated by QENS[10,20,27,28] as well as by molecular dynamics simulation.[11,12]

The results described in this paper serve as a background to further improve the efficiency of the current arsenal of "smart" drug delivery systems available for innovative therapeutic approaches.

Experimental Section

Materials. *N*-Isopropyl acrylamide (NiPAAm) purchased from Aldrich chemicals was recrystallized in *n*-hexane prior to use. All other chemicals were used as received. Poly(vinyl alcohol) with number-average molecular and weight-average molecular weight of 30 ± 5 and 70 ± 10 kg/mol, respectively, D_2O, dextranT40, and FITC-dextran with 4 and 10 kg/mol were purchased from Sigma.

4-(*N*,*N*-Dimethylamino)pyridine (DMAP), glycidyl methacrylate (GMA), and fluorescein isothiocyanate isomer 1 (FITC) were Fluka products. Photoinitiator 2-hydroxy-1-[4-(hydroxyethoxy)phenol]-2-methyl-1-propanone (Irgacure 2959) was a kind gift from Ciba.

Dimethyl sulfoxide (DMSO), inorganic acids, and bases were RPE grade products supplied by Carlo Erba.

The water used was Milli-Q purity grade (18.2 MΩ·cm) produced with deionization apparatus (PureLab) from USF, Elga. Dialysis membranes (cutoff 12 kg/mol) were purchased from Medicell International Ltd. and prepared according to standard procedure.

Methods. ***Preparation of Microgels.*** PVA grafted with glycidyl methacrylate with a 5% degree of substitution (mol/mol repeating units), named PM5, was obtained according to the procedure described elsewhere.[20,28]

Microgels based on PM5 were prepared by adapting a water-in-water emulsion method based on polymer−polymer immiscibility in aqueous solution.[20,21,29,30] In a typical experiment, an aqueous dispersion containing dextran T40 at a concentration of 16% (w/v), PM5 at 2% (w/v), NiPAAm monomer at 1.3% (w/v), and the UV photoinitiator Irgacure 2959 at 0.3% (w/v) was vigorously stirred using an UltraTurrax emulsifier running at 16 000 rpm. After emulsification, PM5 in the dispersed phase was cross-linked by photopolymerization using a 365 nm light source at an intensity of 7 mW/cm^2 for 5 min. The NiPAAm monomers, present in both aqueous phases, were cross-linked in the PM5 containing phase because of the availability of vinyl moiety grafted to PVA chains. The cross-linked PVA/poly(methyl methacrylate-co-*N*-isopropyl acrylamide) microgels were purified by repeated steps of centrifugation and resuspension in Milli-Q water.

Dynamic Light Scattering (DLS). Using a BI-200SM goniometer (Brookhaven Instruments Co.) equipped with a laser source at 532 nm and a BI-9000AT correlation board, the hydrodynamic diameter of thermoresponsive microgels was evaluated as a function of the temperature via the autocorrelation function of the scattered intensity. The temperature of the microgel aqueous suspension was controlled in a range from 20 to 45 °C by an external thermostat. Second-order autocorrelation functions, $g^2(q,t)$, were analyzed using the CONTIN algorithm and a standard software package.

Confocal Laser Scanning Microscopy (CLSM). CLSM observations were performed using a confocal laser scanning microscope (Nikon PCM 2000, Nikon Instruments, Japan) with a Pan Fluor 100×/1.3 oil immersion objective. The 488 nm line of a 100 mW argon ion laser was used for sample fluorescence excitation. Images were collected with a pixel size corresponding to 0.414 μm using the entire field of 512 × 512 pixels. To assess the average pore size using cutoff molecular weight and permeability experiments, suspensions of microgels and FITC-dextran were mixed and examined at room temperature and well above the volume phase transition temperature, i.e., 40 °C. These measurements were performed using a closed chamber stage with a built-in temperature control unit.

Quasielastic Neutron Scattering (QENS). To study the diffusive dynamics of water, microgels containing 80% (w/w) H_2O were analyzed using the IRIS spectrometer[31] at the ISIS pulsed neutron and muon facility (Rutherford Appleton Laboratory, Chilton, UK). Due to the high proton scattering incoherent

SCHEME 1: Chemical Structure of PVA-Based Network

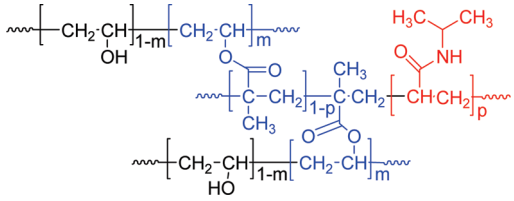

cross section (82.02 barns), the collected spectra are essentially proportional to the self-dynamic structure factor of water and microgel hydrogen atoms. The spectrometer operated using the 002 pyrolytic graphite configuration (energy resolution ΔE_{fwhm} = 17.5 μeV) provides access to a momentum transfer, Q, range from 0.44 to 1.83 Å^{-1} with a dynamic window spanning from −0.35 to 1.2 meV. Empty sample cell and vanadium runs were performed in order to carry out the necessary corrections and calibration, respectively.

The swollen microgel sample was placed in a flat aluminum cell as a slurry after a mild centrifugation of the microgel dispersion in water in order to limit as much as possible the amount of interstitial (bulk) water. The thickness of the sample was 0.1 mm. At this level multiple scattering effects are deemed negligible. Measurements were carried out at 293, 298, 303, 308, 313, and 318 K. With the neutron flux available on IRIS, each data set was collected for 8 h in order to have comparable signal-to-noise ratio for all the samples. The sample temperature was regulated by mounting the sample in a closed-cycle refrigerator (CCR).

Polymer segmental motions were studied by QENS experiments carried out at the high-resolution backscattering spectrometer SPHERES[32] at FRM II, Garching, Germany. The spectrometer provides a Q-range from 0.17 to 1.83 Å^{-1}. For the present experiment, an energy transfer window of ±10 μeV was chosen with a resolution ΔE_{fwhm} of 0.65 μeV. Empty cell and vanadium runs were performed in order to carry out standard corrections and calibration, respectively. The microgel sample at the maximum swelling degree in D_2O, corresponding to a polymer weight fraction of 20%, was placed in a flat aluminum cell as a slurry obtained by mild centrifugation of the microgel suspension. Measurements were carried out from 293 to 313 K. Typically, data were collected for 6 h for each temperature, under vacuum and in a temperature-controlled environment.

Results and Discussion

The thermoresponsive behavior of microgel devices is often accomplished by the inclusion of NiPAAm residues in the network of the hydrogel.[33−35] As already highlighted by Hennink et al.,[36] the "water-in-water" emulsion polymerization method is particularly suitable for biomedical applications where a device is to be embedded in a physiological environment as blood or tissue. The resulting networks, prepared in aqueous media, are not expected to release toxic solvent molecules originating from the microgel fabrication. Recently, we exploited the water-in-water microemulsion technique for the free-radical polymerization of methacrylated PVA chains in the presence of NiPAAm. The aim of that work was the obtainment of a colloidally stable microgel suspension with well-defined spherical shape and having an average diameter of 2 μm with a standard deviation of ±0.5 μm. The polymeric moiety of the microgel network was made by PVA linked by poly(methacrylate-*co*-NiPAAm) copolymers as described in Scheme 1.

Using elemental analysis,[21] the weight of NiPAAm residues incorporated in the polymeric network was found to be 22% (w/w) of the total mass of the polymer network. This corresponds to a copolymerization degree of the NiPAAm residues, p, of 71% (mol/mol of poly(methacrylate-*co*-NiPAAm) residues). The degree of substitution of methacrylic side chains, m, was equal to 5% (mol/mol of PVA repeating unit) determined by ^{1}H NMR (Scheme 1).

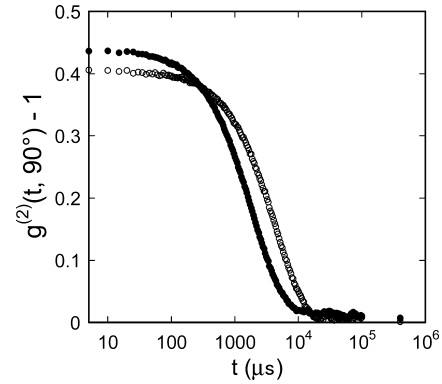

Figure 1. Autocorrelation function of the scattered intensity recorded at 90°. Room temperature (○) and 43 °C (●).

Differential scanning calorimetry, DSC, showed an endothermic transition heat of 13.2 J/g_{NiPAAm} at 34 °C. In addition, dynamic light scattering showed a difference in the hydrodynamic diameter of the microgel particles as a function of temperature.[21] Analysis of the $g^2(t,90°)$ functions shown in Figure 1 gave a hydrodynamic diameter of 1.7 ± 0.2 μm at room temperature and 0.8 ± 0.1 μm at 43 °C, with a shrinking ratio $(V_{h,43°C})/(V_{h,RT})$ = 0.11.

The volume phase transition brought about by heating and cooling was seen to be reversible and without hysteresis. A transition temperature of 33 ± 1 °C was observed in agreement with DSC.

This temperature-dependent response allows the microgel to be used, at least potentially, as a platform for thermally activated drug release. Indeed, the in vitro release of doxorubicin, a well-studied antitumor drug, was enhanced when microgels loaded by doxorubicin were heated from room temperature to physiological temperature.[21] Cytocompatibility was assessed by viability and proliferation tests on fibroblasts in the presence of varying amounts of microgels.[21]

In the present work, size exclusion experiments were performed by CLSM, based on the fluorescence of FITC-dextrans,[37−39] FD. This study revealed that at room temperature FD4 molecules, with a molecular weight of 4 kg/mol and a hydrodynamic diameter of 3 nm, easily permeate the microgel as indicated by the equal fluorescence intensities of the microgel particles and of the surrounding medium (Figure 2a). In a similar permeation experiment, carried out with FD10 molecules, with a molecular weight of 10 kg/mol and a hydrodynamic diameter of 5 nm,[40] the fluorescent probe does not penetrate the network, as indicated by the absence of fluorescence in the microgel particles (Figure 2b). Therefore, it can be inferred that, at room temperature, the pore size of thermoresponsive microgels is between 3 and 5 nm.

A similar approach was used to investigate the pore size of the microgel above the volume phase transition temperature. Figure 3 shows that the fluorescence intensity of the microgel particles at 40 °C, i.e., above VPTT, is not completely dimmed as in the case of FD10 at room temperature, as shown in Figure 2b. The equatorial focal plane of the microgel explored by CLSM allows a view of the microgel core, which leads to the conclusion that the microgel shrinking is coupled with a decrease

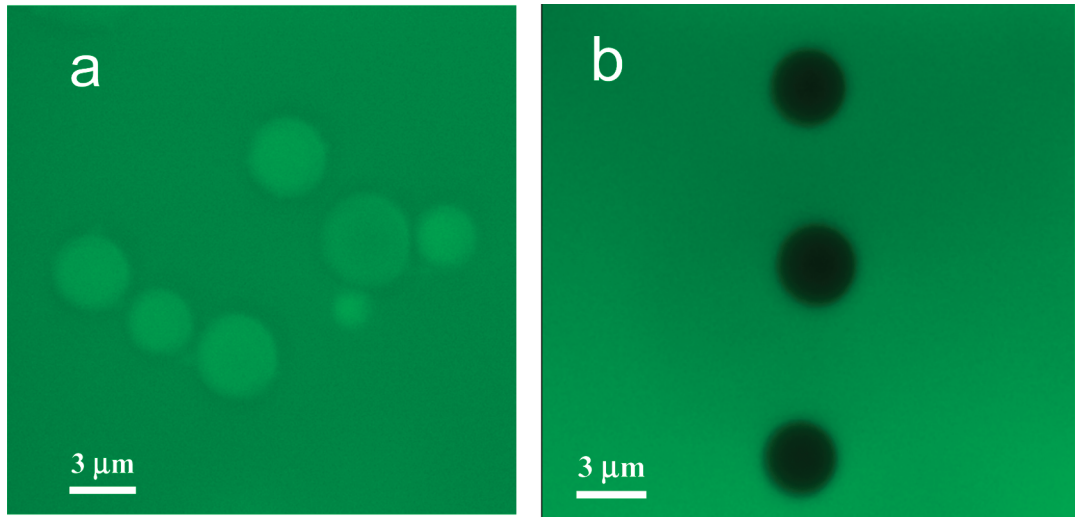

Figure 2. CLSM images of microgel at room temperature with (a) FD4, FITC-dextran (average molecular weight 4 kg/mol), and of (b) FD10, FITC-dextran (average molecular weight 10 kg/mol).

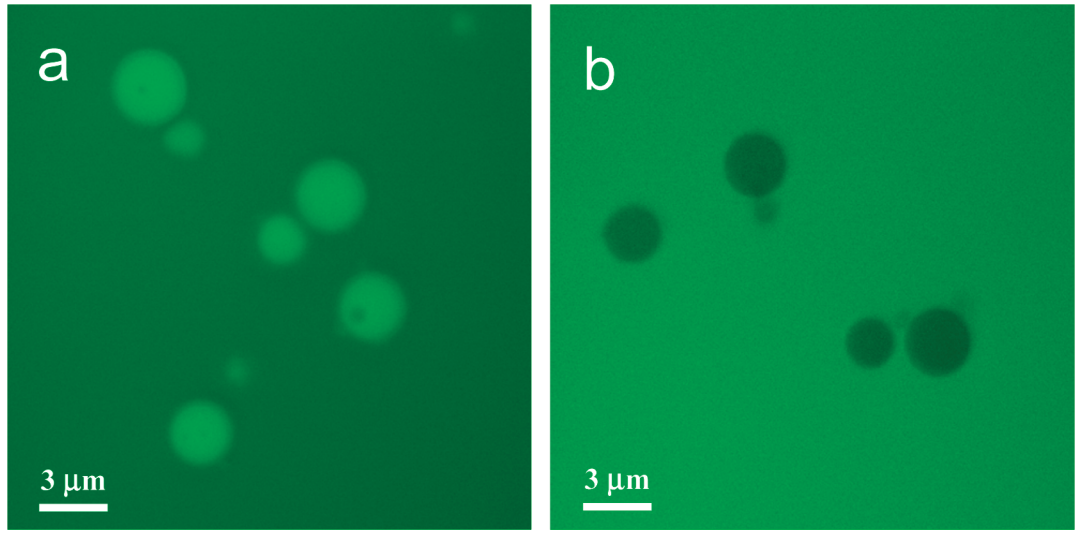

Figure 3. CLSM images of FD4 FITC-dextran molecule (a) at room temperature (shown for comparison) and (b) at 40 °C.

of the network meshes. However, the partial dimming of the fluorescence brought about by FD4 indicates the presence of a pore size distribution of the shrunk network above VPTT, responsible for a not complete exclusion of the FD4 fluorescent probe.

The relaxation processes occurring in hydrated polymeric matrixes are complex and cover many decades in the time (from picoseconds to microseconds), as well as in the space domain with distances ranging from angstroms to nanometers and even micrometers. Such huge space/time intervals cannot be investigated with a single instrument. IRIS, for its static and dynamic characteristics, is well suited to study the diffusion of water in confined systems, whereas the spectrometer SPHERES with its narrow time resolution is an appropriate instrument for investigating segmental dynamics of polymer chains and networks.

The diffusion of water caged in hydrophilic polymer networks is strongly influenced by confinement and results in a supercooling effect. This has been already evidenced by QENS studies[10−12,20,23−27] at nanometer/picosecond space/time scales. It has been noted[10−12,20,27] that a major contribution to this supercooling effect is due to the hydrogen-bond interactions established in the solvation shells close to the polymer chains. In highly hydrated samples, the protons in water molecules can be considered as the only atoms contributing to the overall neutron scattering. For the microgel investigated in this work, the observed scattering law, $S_{obs}(Q,\omega)$, was analyzed by convoluting the instrumental resolution function $R(Q,\omega)$ with the model function S_{inc}:

$$S_{obs}(Q,\omega) = bkg + R(Q,\omega) \otimes S_{inc} \quad (1)$$

with S_{inc} described according to eq 2:

$$S_{inc}(Q,\omega) = \frac{1}{A(Q)}\{pt\delta(\omega) + (1 - pt)[paL_b(Q,\omega) + (1 - pa)L_f(Q,\omega)]\} \quad (2)$$

In eq 2, L_b describes the quasielastic contribution from slow relaxing water molecules associated to the polymer network. In contrast, L_f is used to account for loosely coordinated, fast relaxing water, including interstitial water molecules. The mole fraction of hydrogens belonging to the polymer moiety, pt, is set equal to the degree of hydration as measured experimentally, and pa corresponds to the weight of the slow relaxing water component.

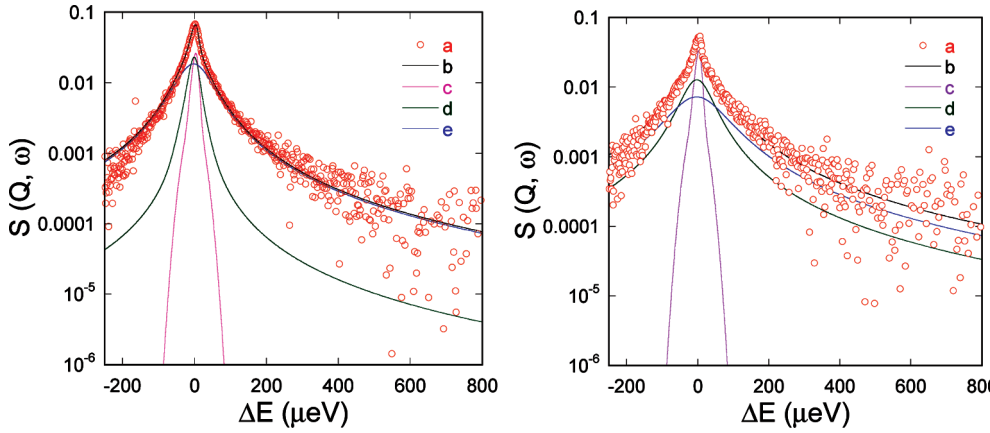

Figure 4. QENS spectra (IRIS) at 293 K (left) and 318 K (right) at $Q = 0.55$ Å^{-1}: (a) experimental data, (b) total fit, (c) elastic polymer component, (d) slow relaxing water component, and (e) fast relaxing water component. For making the fit curves visible, only 30% of the data points are shown.

This model catches only the main features of the system and does not approach its effective structural and dynamic heterogeneities. The presence in the network of domains with different chemical and structural properties, hydrophobicity, and pore size distribution characterizes the complex structure of this microgel. The diffusive behavior of caged water reflects such complexity. However, a detailed description of the single relaxation modes of water in this heterogeneous system would require an exceedingly large number of adjustable parameters of the fitting equation, not justified by the signal-to-noise ratio of the recorded spectra. Also, in analogy with other QENS studies on chemically cross-linked systems containing NiPAAm[10,20,23−26] where similar heuristic descriptions were used, this model neglects rotational contributions of the water molecules, which are broader than the diffusive ones and contribute to a flat background in the energy window considered here.

The quasielastic contribution of the polymeric moiety to the scattering law, S_{obs}, was not included in eq 2 as the results obtained on the same samples with the higher resolution (0.65 μeV) backscattering spectrometer SPHERES showed that the quasielastic peak of the polymer network would be within the IRIS resolution (see below). Moreover, the contribution to the scattering law of faster relaxations such as methyl group rotation from the methacrylic and the acrylamide residues is negligible due to the high degree of hydration of the microgel. As a result, in the model above (eq 2) the localized polymer motions were considered to contribute only to the elastic scattering intensity.

Figure 4 shows $S_{obs}(Q,\omega)$ spectra collected above and below the VPTT of the microgel, together with the relaxation terms L_b and L_f of eq 2 shown separately. Upon heating, an enhancement of the motion associated with the caged water molecules is evident by a broadening of the L_b Lorentzian. At 318 K, at the nm length scale shown (low-Q region), the two terms of eq 2 that describe the relaxation behavior of caged and loosely coordinated water converge toward a single broad Lorentzian (Figure 4, right panel). In our opinion, this is a clear indication of the transition from a dual water dynamic behavior, present at room temperature when strongly associated and loose water molecules both exist in the microgel, to a single fast relaxing water at about 40 °C, above the VPTT. In the whole temperature range explored, the broadening factor of the fast relaxation component L_f provided a diffusion coefficient, estimated from the slope of the L_f broadening vs Q^2 plot in the low-Q limit, and an activation energy close to that found in bulk water at similar temperatures (see Supporting Information).[41,42]

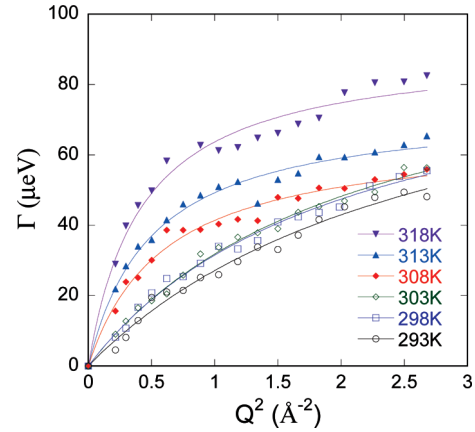

Figure 5. Q-dependence of the line broadening Γ_b of the Lorentzian, L_b, describing the diffusion of "slow" water molecules in the thermoresponsive microgels at different temperatures.

Focusing on the contribution to the total $S_{inc}(Q,\omega)$ of slowly relaxing water molecules, described by the Lorentzian L_b, we analyzed its broadening Γ_b as a function of the scattering vector Q^2 using the random jump diffusion model (Figure 5), eq 3. Here, the diffusion process is described as a set of uncorrelated jumps from one site to another in an unconfined lattice.[43,44]

$$\Gamma_b = \frac{DQ^2}{1 + D\tau Q^2} \tag{3}$$

In eq 3, D and τ are the diffusion coefficient and the residence time of a water molecule in one site, respectively.

According to eq 3, the value of the residence time, τ, is obtained as the inverse of the asymptotic value of the broadening factor of the slow relaxing water Γ_b in the high-Q region. The Q^2-dependence of Γ_b does not allow the evaluation of τ as the asymptotic value is not approached (Figure 5). Therefore, we limited the investigation to the diffusion coefficient, D, which can be determined (eq 3) as the slope of the curve of Γ_b vs Q^2 in the low-Q region.

Table 1 summarizes the temperature dependence of D of the slow relaxing water component.

TABLE 1: Diffusion Coefficient of Strongly Associated Water As a Function of Temperature

temp (K)	$D \times 10^5$ (cm^2 s^{-1})
293	0.56 ± 0.03
298	0.71 ± 0.03
303	0.71 ± 0.03
308	1.7 ± 0.1
313	2.3 ± 0.2
318	3.3 ± 0.3

When compared with the diffusive dynamics of bulk water in the same temperature range, as determined by QENS[42] and by NMR relaxometry[45] (Figure 6), the dynamic behavior of the water molecules associated with the polymer network below VPTT shows evidence of a supercooling effect. This is mainly due to the hydrophilic character of the network.

Comparison of these data to bound-water diffusion coefficients measured using QENS in different types of PVA-based networks[10,11,20] shows that a larger supercooling of water occurs in the present microgels at temperatures lower than VPTT. This can be attributed to the higher chain density of this system enabling a more efficient fixation of the water molecules with the polymeric chains.

Above the VPTT, a marked increase of the diffusion coefficient of water is observed, well above that expected due to thermal enhancement of water diffusion, indicating the recovery of water mobility and the convergence to the diffusion behavior of bulk water.

A qualitatively similar behavior of the diffusion coefficient of water associated with pNiPAAm was recently reported by Osaka et al.[42] in a QENS study of aqueous solutions of this polymer around the lower critical solution temperature.

The temperature dependence of the diffusion coefficient below VPTT provides an activation energy E_a (Figure 7) of 25 kJ/mol, higher than the value of 17.6 kJ/mol reported for bulk water.[46,47] This feature often occurs in water supercooling systems, indicating a strong interaction with the polymer network. The activation energy found below VPTT compares favorably with the values found in different types of PVA-based hydrogels.[10,20,27]

In a dielectric relaxation study of aqueous 10% (w/v) poly(NiPAAm) (molecular weight of 310 kg/mol), an activation energy of 25 kJ/mol was found for the fast mode and attributed to the exchange or dehydration process of water molecules associated with poly(NiPAAm) chains.[48]

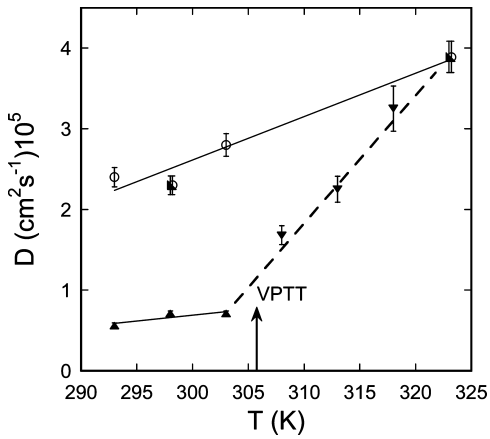

Figure 6. Temperature dependence of the diffusion coefficient of slow relaxing water molecules in thermoresponsive microgel system, below VPTT (▲) and above VPTT (▼), and of bulk water from ref 42 (○), and from ref 45 (right-angle triangles).

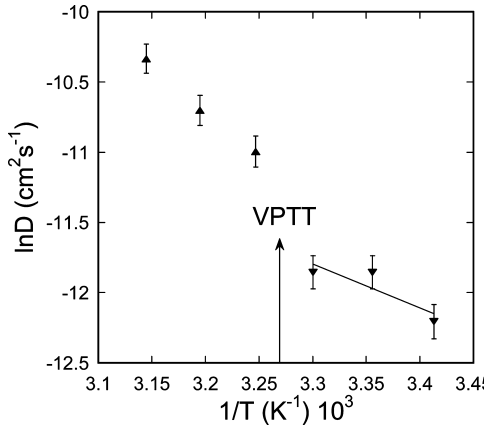

Figure 7. Arrhenius plot of the diffusion coefficient above VPTT (▲) and below VPTT (▼).

Evaluation of an E_a above the VPTT was not attempted because the populations of water associated with the different polymeric components of the network self-exchange as a function of the temperature, with a mixing of their diffusional properties. In this situation an apparent E_a can be retrieved, but its value cannot be linked to a defined kinetic scheme.

Segmental chain motions of the thermoresponsive moiety of the microgel around the VPTT were probed by performing a QENS experiment in D_2O at the neutron backscattering spectrometer SPHERES (FRM-II, Germany).[32] The analysis of the experimental $S_{obs}(Q,\omega)$, was carried out by convoluting the resolution function, $R(Q,\omega)$, with a model that considers the elastic and the quasielastic contributions of the nonexchangeable protons of the polymer network and of closely associated D_2O.

$$S_{obs}(Q,\omega) = \frac{1}{A(Q)}\{\delta(\omega)A_0(Q) + [1 - A_0(Q)]L(Q,\omega)\} \otimes R(Q,\omega) + \text{bkg} \quad (4)$$

In eq 4 the scattering law, S_{obs}, of the polymer network is described by an elastic term, $A_0(Q)$ being the elastic incoherent structure factor (EISF), and a Lorentzian, L, for the quasielastic contribution. D_2O relaxation contributes only to the flat background, bkg, in the energy window accessed by SPHERES (Figure 8).

The geometry of the confined motion of the network hydrogens can be investigated analyzing the Q-dependence of the EISF. Figure 9 shows the fit of the EISF to a modified version of the Volino−Dianoux model[49] which describes the confined motion of protons within a spherical potential of radius R distributed according to a Gaussian law $g(R)$ with average value R_0 and standard deviation σ:[50,51]

$$A_0 = f + (1 - f)\int g(R)\left[\frac{3j_1(QR)}{QR}\right]^2 dR \quad (5)$$

where j_1 is the first-order spherical Bessel function and f is the fraction of "immobile" hydrogens that do not take part to the confined diffusion. R_0 can be considered the radius of a spherical space where protons spatial fluctuations occur. These fluctuations are the result of different dynamic processes occurring in the polymer network, reflecting structural features of the network in the Ångstrom scale as cross-linking degree, hydrophobic/

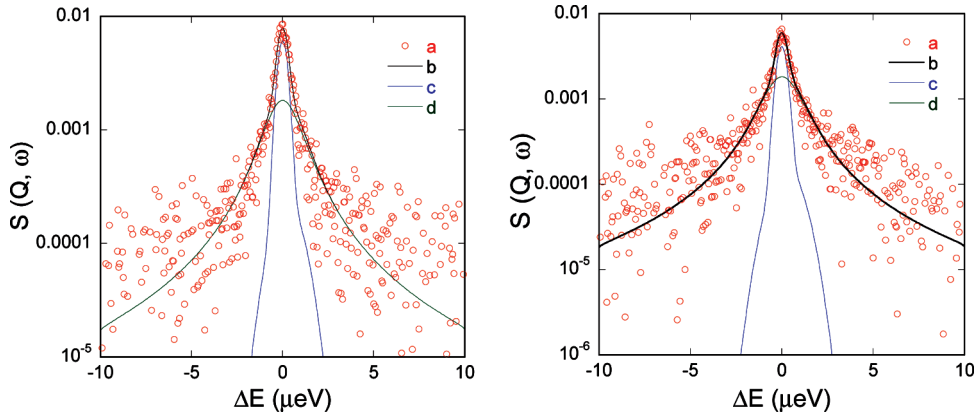

Figure 8. QENS spectra (SPHERES) at 293 K (left) and 313 K (right) at $Q = 1.12$ Å^{-1}: (a) experimental data, (b) total fit, (c) elastic component, and (d) quasielastic component.

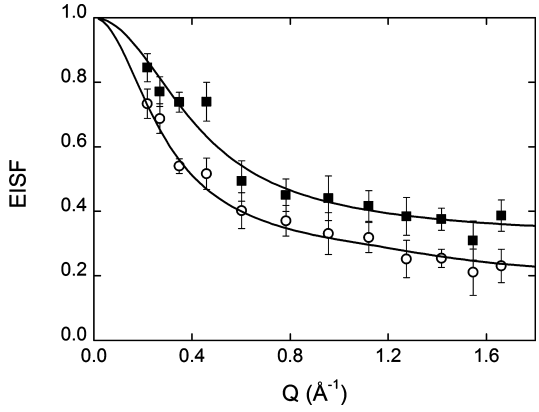

Figure 9. Q-dependence of the elastic incoherent structure factor, EISF, at 293 K (■) and 313 K (○) in thermoresponsive microgel.

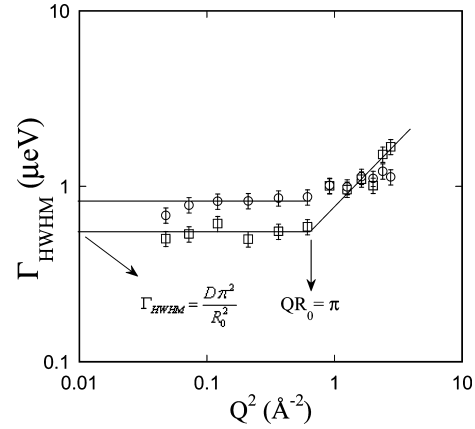

Figure 10. Q^2-dependence of the broadening, Γ_{hwhm}, of the Lorentzian L (eq 4) of the polymer network hydrogens at 293 K (□) and at 313 K (○).

TABLE 2: Parameters Obtained from the Analysis of the EISF of the Thermoresponsive Microgels below and above the VPTT

T (K)	R_0 (Å)	σ (Å)	f
293	3.9 ± 0.1	2 ± 1	0.3 ± 0.1
313	5.1 ± 0.1	3 ± 1	0.18 ± 0.02

hydrophilic balance. A larger R_0 is associated to an average loosening of the network structure.

The values of R_0, σ, and f obtained from the fit are reported in Table 2.

The increase of the EISF parameters with temperature indicates an enhanced mobility of the network hydrogens. This result concerns the overall polymeric network, mainly formed by PVA as NiPAAm residues contribute only for about 20% of the total polymer weight of the microgel. The enhanced mobility of the network therefore refers to the PVA moiety in the microgel, whose dynamic behavior, investigated in previous QENS studies,[10,11,20] indicates an increase of the segmental motions with increasing temperature. Moreover, this behavior has been recently observed in a molecular dynamics simulation study on PVA/poly(methacrylate-*co*-*N*-isopropylacrylamide) chains.[52]

The Q^2-dependence of the broadening Γ_{HWHM} of the Lorentzian describing the relaxation modes of the polymeric moiety above and below the VPTT is reported in Figure 10.

As expected for a confined diffusive dynamics,[49−51,53] Γ_{hwhm} shows a finite nonzero limit as $Q \rightarrow 0$. From this value, a local diffusion coefficient, D, within the confinement volume can be obtained as $\Gamma_{hwhm} = (D\pi^2)/(R_0^2)$. At higher Q values, a departure from a constant behavior is expected since here the dynamics is probed over distances smaller than the confining ones. Only the data recorded at 293 K show a clear inflection point in the Γ_{hwhm} vs Q^2 plot. The inflection indicated by the arrow in Figure 10 is related to the radius of confinement, R_0, according to $QR_0 = \pi$. In this way, a value of R_0 equal to 3.6 Å is obtained. This values compares reasonably well with the one obtained from the EISF (3.9 Å) at the same temperature. Using the R_0 value corresponding to the inflection at 293 K and the asymptotic value of Γ_{hwhm} at low Q, a diffusion coefficient of the segmental motions of the chain of 1.5×10^{-7} cm^2 s^{-1} is obtained. This can be compared to the value of 1.1×10^{-7} cm^2 s^{-1} obtained by Retama et al.[25,26] for the diffusion coefficient of segmental motions of a pNiPAAm network with a degree of cross-linking of 0.25%. In our microgel, despite the higher degree of cross-linking, the slightly higher value of the diffusion coefficient is due to the contribution of the local dynamics of the PVA moiety in the network. This is the dominant (80% by weight) part of the network and is characterized by a higher local mobility as it was shown in our previous QENS study[20] where a PVA-based microgel in the absence of NiPAAm residues displayed a segmental diffusion coefficient of 1×10^{-6} cm^2 s^{-1}. The broadening at 313 K does not show the presence of an inflection in the explored Q range, suggesting a loosening of the structure at temperature higher than VPTT. Within the frame of the model we used, the DQ^2 law (Fickian behavior) can be retrieved only at high QR_0 values (typically $QR_0 \gg 10$), i.e., within distances

where the effect of the confinement becomes negligible. In the SPHERES experiment, the investigated Q range does not extend over values suitable for such evaluation.

Conclusions

This work addresses the structural and dynamic features of a thermoresponsive microgel synthesized using the water-in-water emulsion method. The use of aqueous and cytocompatible materials in this system affords the potential of being used as an injectable microplatform for controlled drug delivery. In a previous papers,[21] we have shown that the incorporation of NiPAAm residues in the PVA-based network invokes a volume phase transition within a physiological temperature range. The transition is associated with the microgel evolving from a swollen state to a collapsed state with a transition temperature at 33 °C. This entropy-driven transition is accompanied by a 50% reduction in the hydrodynamic diameter. It should be noted that the polymerized NiPAAm residues make up only 20% by weight of the overall microgel mass with the remaining 80% being the PVA moiety. The latter is not responsive to the temperature but enables cytocompatibility. In this paper, we focused on those variations of the network architecture at nanoscale which are coupled with the overall size decrease. PVA is known for its hydrophilic character and is often used to maintain high hydration levels in devices when closely interacting with tissues. NiPAAm residues at room temperature are hydrophilic as well. The volume phase transition occurring at physiological temperature is due to the desolvation driven by the increase of hydrophobicity of NiPAAm in these conditions. In agreement with these issues, we found that, around the VPTT, the pore size decreases from about 5 nm to less than 3 nm with a corresponding enhancement of the diffusion dynamics of the water molecules directly associated to the p(NiPAAm) sequences in the network at room temperature.

The overall segmental polymer dynamics shows an intermediate value sitting somewhere between that of a p(NiPAAm) microgel (lower limit) and that of a microgel with identical structure but not containing NiPAAm residues (upper limit). This is expected owing to the presence of the fast relaxation modes introduced by the flexible chains of PVA and to an increase in the overall segmental dynamics of the polymer network. It is still an open issue to assess separately the contributions of p(NiPAAm) and PVA chains within the same network. QENS can help to determine the respective roles of the two polymer moieties in the network dynamics using selective deuteration methods during the microgel fabrication process to incorporate domains with reduced neutron scattering cross sections at controlled cross-linking degree and pore size. The chemical versatility of PVA, the major component of this polymer microgel, supports surface modifications by chemical conjugation with biologically relevant molecules. Suitable biomolecular targeting can be used such that the microgel specifically targets the tissue requesting the pharmacological treatment and promotes the bioadhesion processes to the pathological cells. It is known that tumor cells overexpress the transmembrane protein CD44, a receptor of hyaluronic acid, a polysaccharide naturally occurring in the extracellular matrix. In this view, the polysaccharide, enhancing the adhesion properties of the microgel, promotes the drug bioavailability with an amplification of the cytotoxic effect of the drug on the tumor cell. Micro-/nanodevices responsive to external physical and chemical stimuli are promising supports to new therapeutic approaches.

Acknowledgment. This work was partially funded by MIUR-PRIN project 20077LCNTW. S.G. gratefully acknowledges the international Ph.D. student program of the University of Rome Tor Vergata. The SPHERES experiment has been supported by the European Commission under the Seventh Framework Programme through the Key Action: Strengthening the European Research Area, Research Infrastructures, Contract no.: 226507 (NMI3). The IRIS experiment was performed within Agreement No. 01/901 between CCLRC and CNR.

Supporting Information Available: Figure 1SI: Arrhenius plot of the diffusion coefficients of the fast relaxing water component and of bulk water. This material is available free of charge via the Internet at http://pubs.acs.org.

References and Notes

(1) Zhang, X. Z.; Chu, C. C. *Am. J. Drug Deliv.* **2005**, *3*, 55.
(2) Zhang, J.; Xu, S.; Kumacheva, E. *J. Am. Chem. Soc.* **2004**, *126*, 7908.
(3) Farokhzad, O. C.; Jon, S.; Khademhosseini, A.; Tran, T. T.; LaVan, D. A.; Langer, R. *Cancer Res.* **2004**, *64*, 7668.
(4) Dimitrov, I.; Trzebicka, B.; Muller, A. H. E.; Dworak, A.; Tsvetanov, C. B. *Prog. Polym. Sci.* **2007**, *32*, 1275.
(5) Schmaljohann, D. *Adv. Drug Delivery Rev.* **2006**, *58*, 1655.
(6) Qiu, Y.; Park, K. *Adv. Drug Delivery Rev.* **2001**, *53*, 321.
(7) Berndt, I.; Pedersen, J. S.; Richtering, W. *J. Am. Chem. Soc.* **2005**, *127*, 9372.
(8) Langer, R.; Tirrell, D. A. *Nature* **2004**, *428*, 487.
(9) García Sakai, V.; Arbe, A. *Curr. Opin. Colloid Interface Sci.* **2009**, *14*, 381.
(10) Paradossi, G.; Cavalieri, F.; Chiessi, E.; Telling, M. T. F. *J. Phys. Chem. B* **2003**, *107*, 8363.
(11) Chiessi, E.; Paradossi, G.; Cavalieri, F. *J. Phys. Chem. B* **2005**, *109*, 8091.
(12) Chiessi, E.; Cavalieri, F.; Paradossi, G. *J. Phys. Chem. B* **2007**, *111*, 2820.
(13) Kawaguchi, H. *Prog. Polym. Sci.* **2000**, *25*, 1171.
(14) Fundueanu, G.; Constantin, M.; Ascenzi, P. *Biomaterials* **2008**, *29*, 2767.
(15) Fundueanu, G.; Constantin, M.; Bortolotti, F.; Ascenzi, P.; Cortesi, R.; Menegatti, E. *Macromol. Biosci.* **2005**, *5*, 955.
(16) Henmei, N.; Kawagichi, H.; Endo, T. *Colloid Polym. Sci.* **2007**, *285*, 819.
(17) Costantin, M.; Fundueanu, G.; Bortolotti, F.; Cortesi, R.; Ascenzi, P.; Menegetti, E. *Int. J. Pharm.* **2007**, *330*, 129.
(18) Dufresne, M. H.; Garrec, D. Le.; Sant, V.; Leroux, J. C.; Ranger, M. *Int. J. Pharm.* **2004**, *277*, 81.
(19) Fang, S. J.; Kawaguchi, H. *Colloid Polym. Sci.* **2002**, *280*, 984.
(20) Cavalieri, F.; Chiessi, E.; Villa, R.; Viganò, L.; Zaffaroni, N.; Telling, M. F.; Paradossi, G. *Biomacromolecules* **2008**, *9*, 1967.
(21) Ghugare, S. V.; Mozetic, P.; Paradossi, G. *Biomacromolecules* **2009**, *10*, 1589.
(22) Hirokawa, Y.; Tanaka, T. *J. Chem. Phys.* **1984**, *81*, 6379.
(23) Fernandez-Nieves, A.; Fernandez-Barbero, A.; De las Nieves, F.; Vincent, B. *J. Phys.: Condens. Matter* **2000**, *12*, 3605.
(24) Fernandez-Barbero, A.; Fernandez-Nieves, A.; Grillo, I.; Lòpez Cabarcos, E. *Phys. Rev. E* **2002**, *66*, 051803.
(25) Retama, J. R.; Frick, B.; Seydel, T.; Stamm, M.; Barbero, A. F.; Cabarcos, E. L. *Macromolecules* **2008**, *41*, 4739.
(26) Retama, J. R.; Frick, B.; Seydel, T.; Lopez-Ruiz, B.; Barbero, A. F.; Cabarcos, E. L. *Colloids Surf., A* **2008**, *319*, 149.
(27) Paradossi, G.; Di Bari, M. T.; Telling, M. F.; Turtu, A.; Cavalieri, F. *Physica B* **2001**, *301*, 150.
(28) Cavalieri, F.; Miano, F.; D'Antona, P.; Paradossi, G. *Biomacromolecules* **2004**, *5*, 2439.
(29) Van Dijk-Wolthuis, W. N. E.; Franssen, O.; Talsma, H.; van Stenbergen, M. J.; Kettenes-van den Bosh, J. J.; Hennink, W. E. *Macromolecules* **1995**, *28*, 6317.
(30) Van Dijk-Wolthuis, W. N. E.; Kettenes-van den Bosh, J. J.; van der Kerk-van Hoof, A.; Hennink, W. E. *Macromolecules* **1997**, *30*, 3411.
(31) www.isis.stfc.ac.uk/instruments/iris/.
(32) www.jcns.info/jcns_spheres.
(33) Schild, H. G. *Prog. Polym. Sci. (Oxford)* **1992**, *17*, 163.
(34) Maeda, T.; Akasaki, Y.; Yamamoto, K.; Aoyagi, T. *Langmuir* **2009**, *25*, 9510.
(35) Garcia, A.; Marquez, M.; Cai, T.; Rosario, R.; Hu, Z.; Gust, D.; Hayes, M.; Park, C.-D. *Langmuir* **2007**, *23*, 224.
(36) Franssen, O.; Hennink, W. E. *Int. J. Pharm.* **1998**, *168*, 1.

(37) Ibarz, G.; Dahne, L.; Donath, E.; Mohwald, H. *Chem. Mater.* **2002**, *14*, 4059.
(38) Ibarz, G.; Dahne, L.; Donath, E.; Mohwald, H. *Macromol. Rapid Commun.* **2002**, *23*, 474.
(39) Tong, W.; Gao, C.; Möhwald, H. *Chem. Mater.* **2005**, *17*, 4610.
(40) Torak, M. S.; McKenna, B. J.; Waite, J. H.; Stucky, G. D. *Chem. Mater.* **2007**, *19*, 4263.
(41) Texeira, J.; Bellissent-Funel, M.-C.; Chen, S. H.; Dianoux, A. J. *Phys. Rev. A* **1985**, *31*, 1913.
(42) Osaka, N.; Shibayama, M.; Kikuchi, T.; Yamamuro, O. *J. Phys. Chem. B* **2009**, *113*, 12870.
(43) Bée, M. In *Quasielastic Neutron Scattering*; Hilger, A., Ed.; Elsevier Science: Bristol, UK, 1988.
(44) Singwi, K. S.; Sjolander, A. *Phys. Rev.* **1960**, *119*, 863.
(45) Krynicki, K.; Green, C. D.; Sawyer, D. W. *Faraday Discuss. Chem. Soc.* **1978**, 199.
(46) Mills, R. *J. Phys. Chem.* **1973**, *77*, 685.
(47) Sun, P.; Li, B.; Wang, Y.; MA, J.; Ding, D.; He, B. *Eur. Polym. J.* **2003**, *39*, 1045.
(48) Ono, Y.; Shikata, T. *J. Am. Chem. Soc.* **2006**, *128*, 10030.
(49) Volino, F.; Dianoux, A. J. *Mol. Phys.* **1980**, *41*, 271.
(50) Di Bari, M. T.; Gerelli, Y.; Sonico, F.; Deriu, A.; Cavatorta, F.; Albanese, G.; Colombo, P.; Fernandes-Alonso, F. *Chem. Phys.* **2008**, *345*, 239.
(51) Nogales, A.; Ezquerra, T. A.; Batallan, F.; Frick, B.; Lopez-Cabarcos, E.; Baltá-Calleja, F. J. *Macromolecules* **1999**, *32*, 2301.
(52) Chiessi, E.; Lonardi, A.; Paradossi, G. *J. Phys. Chem. B* **2010**, *114*, 8301.
(53) Hall, P. L.; Ross, D. K. *Mol. Phys.* **1981**, *42*, 673.

JP100962P